Scopoletin negatively regulates the HOG pathway and exerts antifungal activity against *Botrytis cinerea* by interfering with infection structures, cell wall, and cell membrane formation

Xiaojun Yuan[1], Fugen Yang[1], Yameng Wang[1], Shaoxuan Li[2,3], Demeng Zhang[3], Wenxing Liang[1*] and Qianqian Yang[1*]

Abstract

Botrytis cinerea is the causative agent of gray mold, a fungal disease affecting a broad array of food crops and resulting in considerable agricultural and economic losses. Currently, chemical fungicides are the most effective control measure, but this practice is challenged by the growing resistance of pathogens to these fungicides. Scopoletin, a major phytoalexin of tobacco plants, has shown promise as an antifungal treatment. Here, we found that scopoletin was effective against *B. cinerea* infection of tomato leaves. It inhibited mycelial growth and conidial germination of *B. cinerea* and disrupted cell wall, cell membrane, and infection structure formation. Transcriptomic analysis identified 3495 differentially expressed genes in response to scopoletin treatment. Interestingly, scopoletin seems to deactivate the HOG pathway of *B. cinerea*. The growth defect caused by hyperactivation of the pathway, such as iprodione treatment and deletion of *BcPtc1*, the negative regulator of this pathway, was partly rescued by scopoletin. Moreover, it could downregulate phosphorylation levels of BcSak1 treated with iprodione and NaCl. In addition, the control efficiency of triadimefon was significantly increased by scopoletin. Thus, scopoletin is a promising, naturally derived, and sustainable treatment for gray mold, especially when combined with triadimefon.

Keywords *Botrytis cinerea*, Fungicide, Scopoletin, Phytoalexin, HOG pathway

*Correspondence:
Wenxing Liang
wliang790625@163.com
Qianqian Yang
qyang@qau.edu.cn
[1] College of Plant Health and Medicine, Qingdao Agricultural University, Qingdao 266109, China
[2] Qingdao Academy of Agricultural Science, Qingdao 266100, China
[3] Key Laboratory of Seaweed Fertilizers, Ministry of Agriculture and Rural Affairs, Qingdao Brightmoon Seaweed Group Co. Ltd., Qingdao 266400, China

Background

Botrytis cinerea, the causative agent of gray mold, is a necrotrophic plant pathogen that can infect a diverse array of host plants during both pre- and post-harvest phases, leading to significant economic losses (Williamson et al. 2007). Currently, chemical treatment is considered the most effective method of controlling gray mold, with growers and processors employing several types of fungicides, including phenylpyrroles, quinone outside inhibitors, hydroxyanilides, dicarboximides, anilinopyrimidines, and benzimidazoles (Yin et al. 2016; Adnan et al. 2019). However, the continued use and

Yuan *et al. Phytopathology Research*   (2024) 6:1

Page 2 of 14

overuse of chemical fungicides have led to the evolution of fungicide-resistant pathogen strains, ineffective disease control, food safety concerns, agricultural losses, and environmental issues (Yin et al. 2016). Therefore, there is an urgent need for sustainable and effective control strategies for gray mold.

Phytoalexins are a group of natural substances that plants produce in response to stress, both biotic and abiotic, and they have the potential to provide broad-spectrum protection against fungal pathogens. These substances are low molecular mass secondary metabolites that exhibit antimicrobial properties. One such phytoalexin that is of particular interest is scopoletin, also known as 6-methoxy-7-hydroxycoumarin (Fig. 1a). Scopoletin is a phytoalexin common in *Nicotiana tabacum, Sinomonium acutum*, and *Melia azedarach* L. (Shaw et al. 2003; Carpinella et al. 2005). In fact, the resistance of different tobacco cultivars to gray mold is correlated with the amount of scopoletin and pathogenesis-related proteins present in plant tissues (El Oirdi et al. 2010).
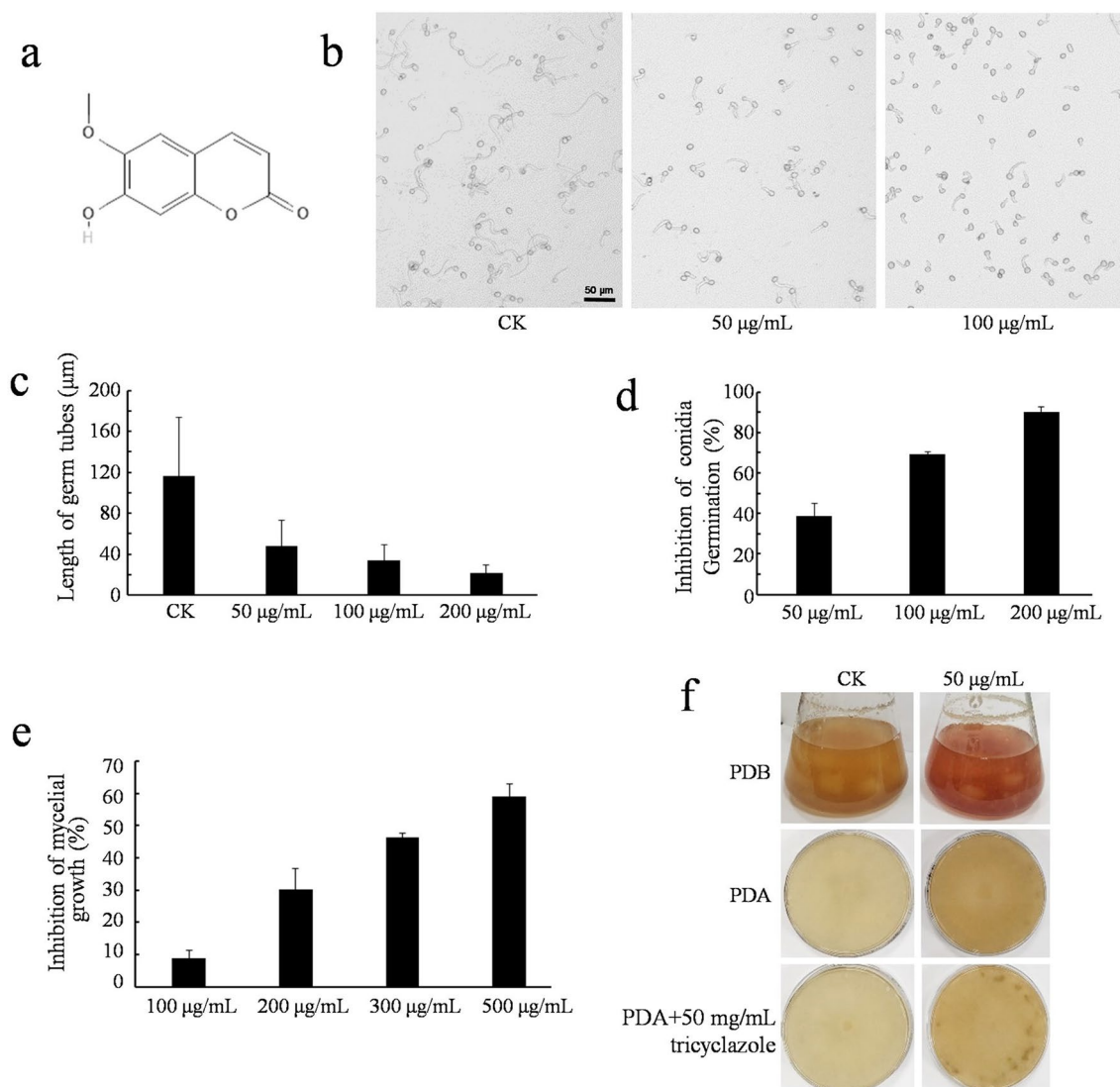

Fig. 1 Scopoletin is effective against *B. cinerea*. **a** Structure of scopoletin. **b** Conidia germination of *B. cinerea* with/without scopoletin. Conidia were collected and suspended in 1/2 PDB with/without scopoletin. The pictures were taken after 3 h of incubation at 25℃. **c** Inhibition of germ tubes by scopoletin. Lengths of more than 50 germ tubes were measured under a microscope. **d** Inhibition of conidia germination by scopoletin. **e** Inhibition of mycelial growth of *B. cinerea* by scopoletin. **f** Scopoletin caused increased pigmentation of *B. cinerea*. Mycelia of *B. cinerea* were treated with 50 μg/mL scopoletin for 3 h after being cultured in PDB medium for 36 h. *B. cinerea* was cultured on PDA plates with/without 50 μg/mL scopoletin. The pictures were taken after 8 days of incubation at 25℃

Moreover, scopoletin has been found to accumulate in tobacco in response to tobacco mosaic virus infection, effectively inducing localized systemic resistance (Costet et al. 2002).

The efficacy of scopoletin as an antifungal agent has been studied in various fungi. Its fungistatic activity against *Phakopsora pachyrhizi*, the causative agent of Asian soybean rust, was confirmed through in vitro experimentation (Beyer et al. 2019). In wild tobacco, scopoletin was found to exhibit strong antifungal activity against *Alternaria alternata* in both in *vitro* and in *vivo* assays, apparently through its involvement in jasmonate signaling (Sun et al. 2014). Research on *Fusarium verticillioides* found the minimum inhibitory concentration (Michielse et al. 2011) of scopoletin to be 1.50 mg/mL. Scopoletin has also shown antifungal activity against *Candida* species by disrupting biofilm formation (Lemos et al. 2020). Aside from its antifungal properties, scopoletin has potential as a pharmacological agent due to its antioxidant activity, which may provide therapeutic benefits for disorders caused by an imbalance of reactive oxygen species (Choquer et al. 2004; Parra et al. 2018). Additionally, scopoletin has also been found to exhibit anti-inflammatory, anticancer, and neuroprotective activities (Antika et al. 2022).

In this study, we sought to determine the sensitivity of *B. cinerea* to scopoletin and explore its possible mechanism of action. We found that scopoletin effectively inhibited *B. cinerea* mycelial growth, conidia germination, and infection structure formation. Transcriptomic analysis of *B. cinerea* exposed to scopoletin identified 3495 differentially expressed genes (DEGs), including 1285 upregulated genes and 2210 downregulated genes. Thirteen of these mentioned DEGs were found to be involved in *B. cinerea* virulence. Finally, scopoletin was found to regulate the high-osmolarity glycerol (HOG) pathway and destabilize cell walls, cell membranes, and infection structure formation in *B. cinerea*. Interestingly, scopoletin could deactivate the HOG pathway and increase the control efficiency of triadimefon against *B. cinerea*. Based on these results, we propose that scopoletin is a promising candidate for fungicide development.

Results

Scopoletin inhibits conidial germination and mycelial growth of *B. cinerea*

To test the antifungal activity of scopoletin, we quantified the conidial germination rates of *B. cinerea* B05.10 in response to scopoletin treatment. As shown in Fig. 1, not only was the conidial germination rate significantly reduced by scopoletin, but the length of germ tubes was significantly shorter than the control treatment (Fig. 1b, c). The half maximal effective concentration (EC_{50}) of scopoletin for inhibiting conidial germination rate was found to be 66.1 ± 12.9 μg/mL (Fig. 1d). Furthermore, mycelial growth of *B. cinerea* B05.10 was significantly inhibited by scopoletin treatment, with the EC_{50} estimated to be 392 ± 26.2 μg/mL (Fig. 1e).

In addition, scopoletin caused increased pigmentation of *B. cinerea*, and mycelia treated with 50 μg/mL scopoletin were observed with darker pigment compared to the control and this result was observed on both liquid medium (PDB) and potato dextrose agar (PDA) plates (Fig. 1f). To test whether the pigment is melanin, B05.10 was incubated on PDA supplemented with 50 mg/mL tricyclazole, which is an inhibitor of fungal melanin biosynthesis (Thompson et al. 2000). However, the results showed that the darker pigment formation was not affected by tricyclazole, indicating that the dark pigment is not melanin.

Inhibition ability of gray mold by scopoletin

The ability of scopoletin to control gray mold on tomato leaves was tested. At a treatment rate of 50 μg/mL, scopoletin was able to significantly reduce the size of disease lesions caused by *B. cinerea* B05.10 on tomato leaves (Fig. 2a). Moreover, at a treatment rate of 100 μg/mL, only primary disease lesions were observed on tomato leaves (Fig. 2a). In addition, the protective effect of scopoletin was also tested and tomato plants treated with

(See figure on next page.)

Fig. 2 Scopoletin could inhibit *B. cinerea* infection. **a** Symptoms of tomato leaves with *B. cinerea* (10^5 conidia/mL) infection following treatment with 50 μg/mL or 100 μg/mL scopoletin. The upper lanes of tomato leaves were unpretreated with scopoletin, while the lower lanes of tomato leaves were pretreated with 50 μg/mL or 100 μg/mL scopoletin for 2 h. The conidia suspension without treatment was used as the control (nontreatment, NT). The diameters of disease lesions on tomato leaves were measured after 3 d of incubation. **b** Onion epidermis penetration by conidia of *B. cinerea* treated with 50 μg/mL or 100 μg/mL scopoletin. The photos were taken after 16 h of inoculation. **c** Scopoletin reduces appressorium formation in *B. cinerea*. Conidia were harvested and suspended in 10 mM fructose. The photos were taken after 8 h of inoculation at 25℃. The appressoria were indicated with red arrows. **d** Scopoletin impairs infection cushion development in *B. cinerea*. Mycelium plugs taken from the edge of the 2-day-old culture of *B. cinerea* were placed on clean slides and incubated at 25℃ for 36 h. The red curves indicated the edge of mycelium plugs, and the blue curves indicated the sites that are 600 μm away from the edge of mycelium plugs. **e** Number of infection cushions at the sites 600 μm away from the mycelium plugs. Values on the bars followed by different letters are significantly different at $P = 0.05$
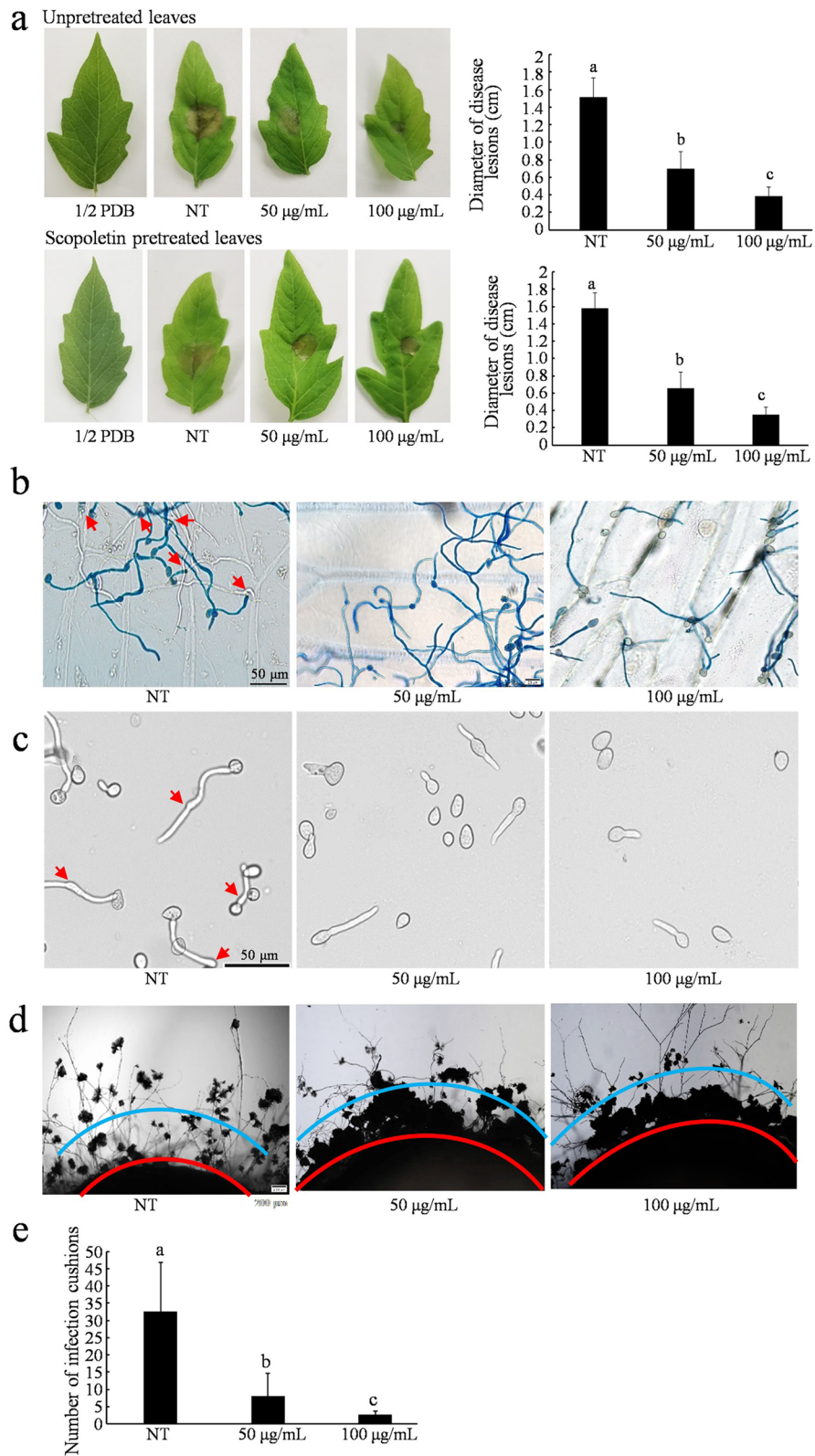
Fig. 2 (See legend on previous page.)

Yuan *et al. Phytopathology Research*   (2024) 6:1

Page 5 of 14

scopoletin 2 h before *B. cinerea* inoculation had similar control effect against *B. cinerea* (Fig. 2a).

To further explore the control mechanism of scopoletin in detail, an infection-related morphogenesis assay was conducted. As shown in Fig. 2b, scopoletin was able to inhibit penetration of *B. cinerea* B05.10 into onion epidermal cells (Fig. 2b). Based on these results, infection structure development of *B. cinerea* with/without scopoletin was examined. As shown in Fig. 2c, appressorium formation was significantly inhibited under scopoletin treatment. In addition, most infection cushions were observed around the mycelium plugs, while only a few cushions were found at sites nearly 600 μm away from the mycelium plugs under scopoletin treatment (Fig. 2d, e). These results indicate that scopoletin can interfere with the development of infection structures.

RNA-Seq, transcriptome assembly, and analysis of differentially expressed genes

To explore the mechanism by which scopoletin exerts antifungal effect against *B. cinerea* B05.10, transcriptomic sequencing was carried out. More than 40,000,000 reads were obtained across all six tested samples, and more than 95% of these reads were mapped to the reference genome (Additional file 1: Table S1).

A total of 3495 differentially expressed genes (DEGs) were identified, with 1285 being upregulated and 2210 downregulated (Fig. 3a and Additional file 2: Table S2). Heatmap clustering of 3495 DEGs indicated that the expression pattern of scopoletin-challenged *B. cinerea* B05.10 was significantly different from that of control cultures (Fig. 3b). Reverse transcription quantitative PCR (RT-qPCR) was used to validate the expression of seven DEGs, which were found to be consistent with the RNA-seq results (Fig. 3c).

The DEGs were analyzed using GO (Gene Ontology) and KEGG (Kyoto Encyclopedia of Genes and Genomes) annotation to identify gene functions and pathways (Fig. 3d and Additional file 3: Table S3). Of these, nine GO terms were associated with biological processes (BPs), including DNA replication (GO:0006260), DNA-dependent DNA replication (GO:0006261), carbohydrate metabolic process (GO:0005975), DNA metabolic process

(GO:0006259), DNA replication initiation (GO:0006270), DNA strand elongation involved in DNA replication (GO:0006271), DNA strand elongation (GO:0022616), double-strand break repair (GO:0006302), and response to stress (GO:0006950); five were associated with cellular components (CC), including of integral component of membrane (GO:0016021), intrinsic component of membrane (GO:0031224), replication fork (GO:0005657), chromosome (GO:0005694), and chromosomal part (GO:0044427); and two were associated with molecular functions (MF), both related to hydrolase activity (GO:0004553 and GO:0016798).

In plants, oxidative burst (OB) is a rapid and efficient defensive strategy (Federica Zaninotto and Delledonne 2006). In response to host OB and hypersensitive response (HR), pathogens have developed strategies to enzymatically detoxify reactive oxygen species (ROS) (Choquer et al. 2004). Here, we found that scopoletin treatment resulted in the altered expression of 13 peroxidase genes (GO:0004601) and 15 genes that are related to antioxidant activity (GO:0016209) (Table 1).

In addition, a total of 11 significant KEGG pathways were identified (Fig. 3e and Additional file 4: Table S4), including DNA replication (bfu03030), mismatch repair (bfu03430), cell cycle-yeast (bfu04111), meiosis-yeast (bfu04113), homologous recombination (bfu03440), pentose and glucuronate interconversions (bfu00040), starch and sucrose metabolism (bfu00500), base excision repair (bfu03410), cyanoamino acid metabolism (bfu00460), nucleotide excision repair (bfu03420), and fructose and mannose metabolism (bfu00051).

Scopoletin destabilizes *B. cinerea* cell walls and cell membranes

The GO enrichment analysis indicated that scopoletin treatment caused dysregulation of cell membrane biosynthesis (GO:0016021 and GO:0031224). Further analysis revealed the downregulation of several genes involved in ergosterol in response to scopoletin treatment, including *BcErg1* (−2.43), *BcErg3* (−1.54), *BcErg5* (−1.10), and *BcErg8* (−1.06). Furthermore, scopoletin-treated *B. cinerea* B05.10 exhibited propidium iodide (PI) staining compared to control cultures in both mycelium and

(See figure on next page.)

Fig. 3 RNA-seq analysis of *B. cinerea* treated with 10 μg/mL scopoletin. **a** Number of differentially expressed genes (DEGs) between the control cultures (BCK) and *B. cinerea* cultures treated with 10 μg/mL scopoletin (Bsco). **b** Heatmap of the DEGs between the control cultures (BCK1, BCK2, and BCK3) and cultures treated with 10 μg/mL scopoletin (Bsco1, Bsco2, and Bsco3). **c** Seven DEGs were selected for RT-qPCR validation. **d** Gene Ontology (GO) enrichment analysis. The size and color of the dots indicate the number of DEGs and the significance of the GO terms, respectively. The significant GO terms are shown in red letters. **e** Kyoto Encyclopedia of Genes and Genomes (KEGG) pathway enrichment analysis. The size and color of the dots indicate the number of DEGs and the significance of the KEGG pathways, respectively. The significant KEGG pathways are shown in red letters
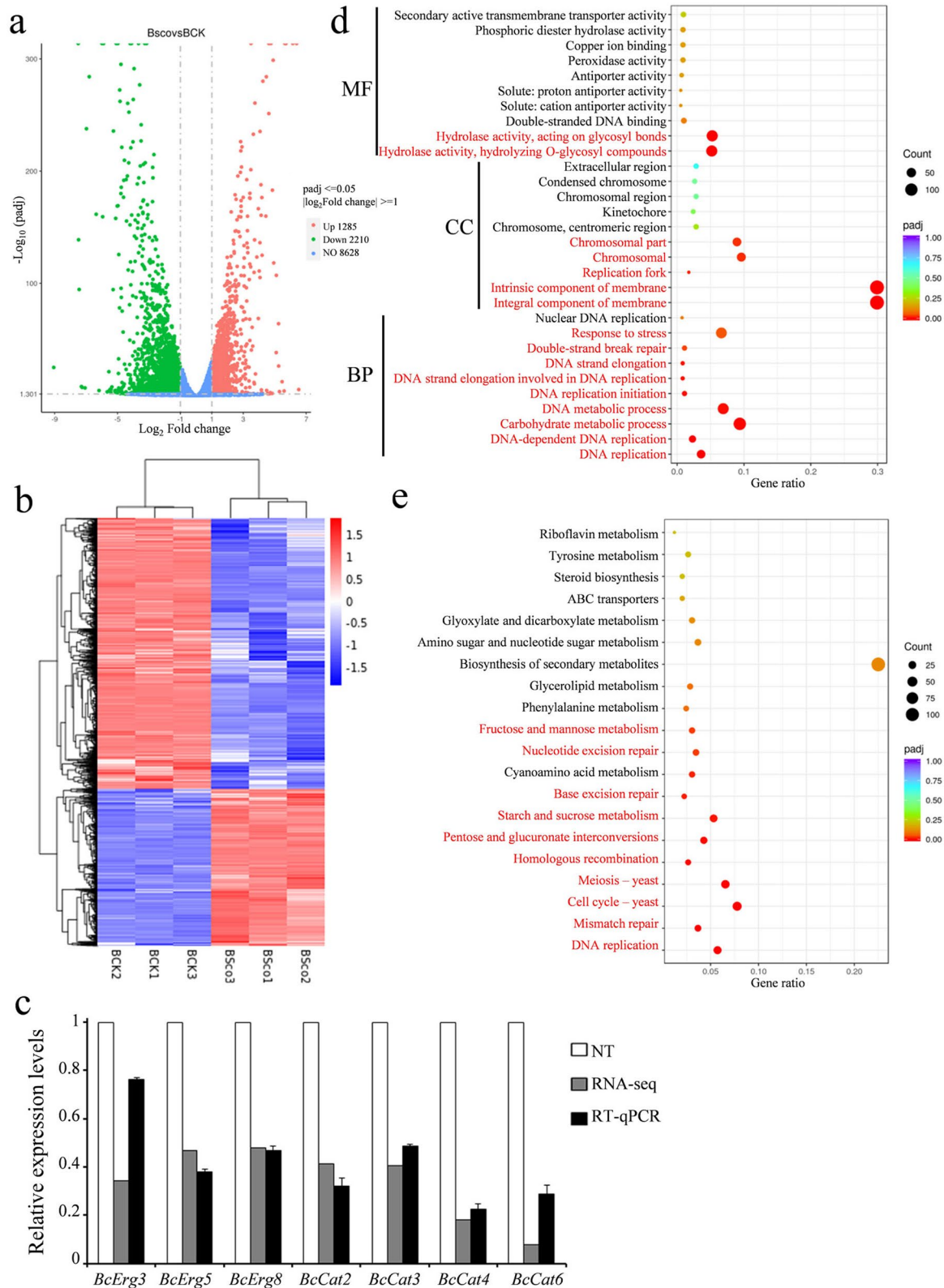
Fig. 3 (See legend on previous page.)

Table 1 DEGs involved in the peroxidase activity and antioxidant activity of *B. cinerea*

Gene_id	Genes	log$_2$Fold change
Bcin05g04580	*Bccat6*	−3.74
Bcin13g05720	*Bcprd1*	−2.93
Bcin09g03760	*Bcprd9*	−2.70
Bcin05g00730	*Bccat4*	−2.47
Bcin03g07850	*Bcprd10*	−2.23
Bcin05g00590	*Bcprd4*	−2.07
Bcin03g01920	*Bccat5*	−1.52
Bcin06g04520	*Bccat3*	−1.31
Bcin11g06450	*Bccat2*	−1.28
Bcin05g02680	*Bctrr1*	1.11
Bcin03g01480	*Bcgpx3*	1.17
Bcin03g03390	*Bcsod1*	1.20
Bcin13g03680	*Bcprd11*	1.42
Bcin10g02560	*Bcprd7*	1.44
Bcin02g03060	*BcppoA80*	1.73

conidia (Fig. 4a, b). The treatment also resulted in the dysregulation of cell wall biosynthesis, acting to upregulate several chitin synthase genes, including *BcCHSI* (3.06), *BcCHSIIIa* (2.17), *BcCHSII* (2.15), and *BcCHSVII* (1.11). However, similar fluorescence was detected in both scopoletin-treated and untreated samples using calcofluor white stain assay, which indicated chitin biosynthesis was not affected by scopoletin (Fig. 4c). In addition, mycelium treatment with scopoletin resulted in a significant increase in protoplast formation in fresh hyphae treated with 0.25% lysing enzymes (Sigma-Aldrich) for 2 h (Fig. 4d). Furthermore, *Bcgas2*, one of β-1,3-glucanosyltransferase Gel family which could elongate cell wall β-1,3-glucan, is significantly downregulated (− 1.84) (Zhao et al. 2014), indicating that another component of cell wall, glucan is interfered by scopoletin. Taken together, scopoletin appears to destabilize fungal cell walls and cell membranes.

Scopoletin increases the control efficiency of triadimefon
Since scopoletin caused dysregulation of ergosterol biosynthesis, the sensitivity of *B. cinerea* to triadimefon, a sterol demethylation inhibitors (DMIs) with/without scopoletin was tested. The results, shown in Fig. 5a, indicate that scopoletin significantly increased the control efficiency of triadimefon.

Scopoletin regulates the high-osmolarity glycerol (HOG) pathway of *B. cinerea*
The GO enrichment analysis indicated that there was a significant upregulation of the stress response (GO:0006950) in response to scopoletin treatment.

Specifically, two components of the HOG pathway—*BcSho1* and *BcPtc1*, which regulate stress response in fungi, were notably upregulated in response to scopoletin treatment with a respective increase of 1.65 and 1.10, respectively (Yang et al. 2013; Ren et al. 2019). Therefore, scopoletin may have a role in regulating the HOG pathway of *B. cinerea*.

Since dicarboximide fungicides and osmotic stress have been shown to activate the HOG pathway in *B. cinerea* (Liu et al. 2008), we first examined the sensitivity of *B. cinerea* to iprodione and NaCl with/without scopoletin. Surprisingly, scopoletin partly rescued the growth defect of *B. cinerea* on iprodione and NaCl plates (Fig. 5a). In order to further explore the regulatory mechanism of scopoletin in HOG pathway, deletion mutant of *BcPtc1*, a negative regulator of HOG pathway was also tested. As previously reported, Δ*BcPtc1* showed excessive activation of the pathway and caused severe growth defects (Yang et al. 2013). As shown in Fig. 5b, the growth defect was partly rescued by scopoletin.

Finally, we examined the phosphorylation status of BcSak1, the core element of the HOG pathway in scopoletin-challenged *B. cinerea* B05.10. In consist with the previous study (Yang et al. 2013), BcSak1 phosphorylation was increased in response to NaCl and iprodione, and scopoletin significantly reduced the phosphorylation levels (Fig. 5c). These results indicate that scopoletin acts to deactivate the HOG pathway.

Analysis of *B. cinerea* virulence factors
The expression patterns of 41 virulence-associated genes, including 23 upregulated genes and 18 downregulated genes, were significantly altered in response to scopoletin treatment (Table 2). Among these genes, *Bcaba2*, involved in ABA biosynthesis (Siewers et al. 2006), exhibited the highest upregulation. On the other hand, *Bcmfs1*, which encodes a major facilitator superfamily transporter (Hayashi et al. 2002), exhibited the greatest downregulation. As mentioned above, four chitin synthase genes (*BcCHSI*, *BcCHSIIIa*, *BcCHSII*, and *BcCHSVII*) were also significantly upregulated.

Discussion
Since *B. cinerea* is responsible for considerable agricultural and economic losses, effective strategies for controlling gray mold are in high demand (Williamson et al. 2007). Chemical fungicide application remains the most effective strategy; however, the limited number of effective fungicides and increasing levels of fungicide resistance among pathogenic strains have made this practice challenging (Fillinger and Elad 2016). Thus, effective and sustainable antifungal treatment options are badly needed. In this study, we found that the naturally
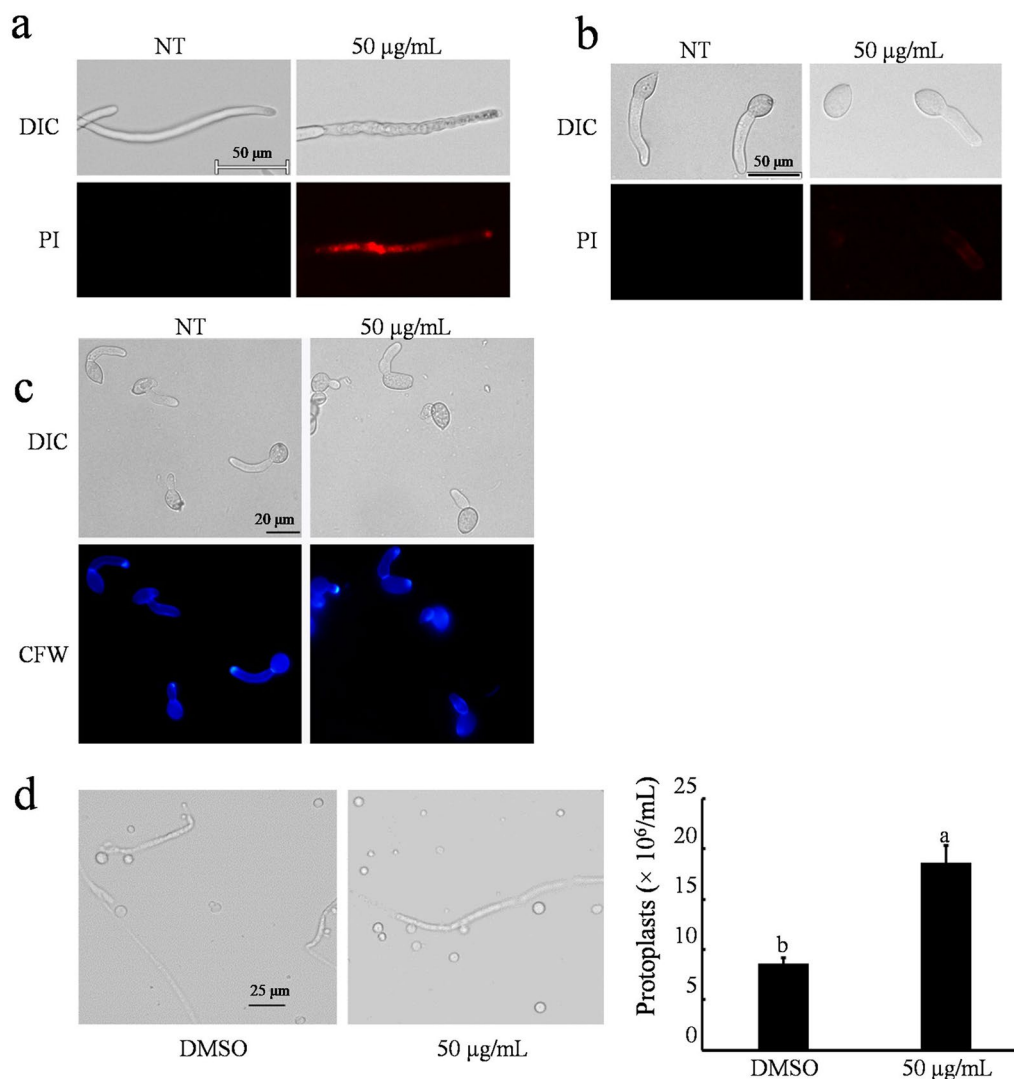
Fig. 4 Scopoletin affects cell wall and cell membrane formation. **a** Propidium iodide (PI) fluorescence assay of *B. cinerea* mycelia. Mycelia were treated with 50 μg/mL scopoletin for 3 h. **b** PI fluorescence assay of *B. cinerea* conidia. Conidia were harvested and treated with 50 μg/mL scopoletin for 3 h. **c** Calcofluor white (CFW) staining of *B. cinerea* conidia. Conidia were harvested and treated with 50 μg/mL scopoletin for 3 h. **d** Scopoletin treatment significantly increased the protoplast formation of *B. cinerea*. Fresh hyphae were first treated with 50 μg/mL scopoletin for 3 h, and then incubated for 2 h in 0.6 M KCl containing 0.25% lysing enzymes before microscopic examination. Values on the bars followed by different letters are significantly different at $P = 0.05$

occurring phytoalexin scopoletin was effective against *B. cinerea* infection in tomato leaves. Specifically, we found that scopoletin can inhibit mycelia growth, conidial germination, and the formation of infection structures in *B. cinerea*. Additionally, it disrupts cell wall and cell membrane formation and ROS homeostasis.

The antifungal mechanism of scopoletin against *B. cinerea* was explored through RNA-seq analysis. Over 3000 DEGs were identified, with approximately one-third upregulated and two-thirds downregulated. Of these DEGs, 16 GO terms and 11 KEGG pathways were

identified. Scopoletin treatment affected the gene expression levels of several DNA-related processes, including elongation, replication, initiation, repair, and metabolism. These findings provide evidence for the antifungal activity of scopoletin against *B. cinerea*.

As shown in Fig. 1f, scopoletin caused increased pigmentation of *B. cinerea*. The main pigment in *B. cinerea* is 1,8-dihydroxynaphthalene (DHN) melanin, which is catalyzed by polyketide synthases (PKS, BcPKS13, and BcPKS12), yellowish-green hydrolase 1 (YGH1 and BcYGH1), two reductases (BcBRN1 and BcBRN2) and
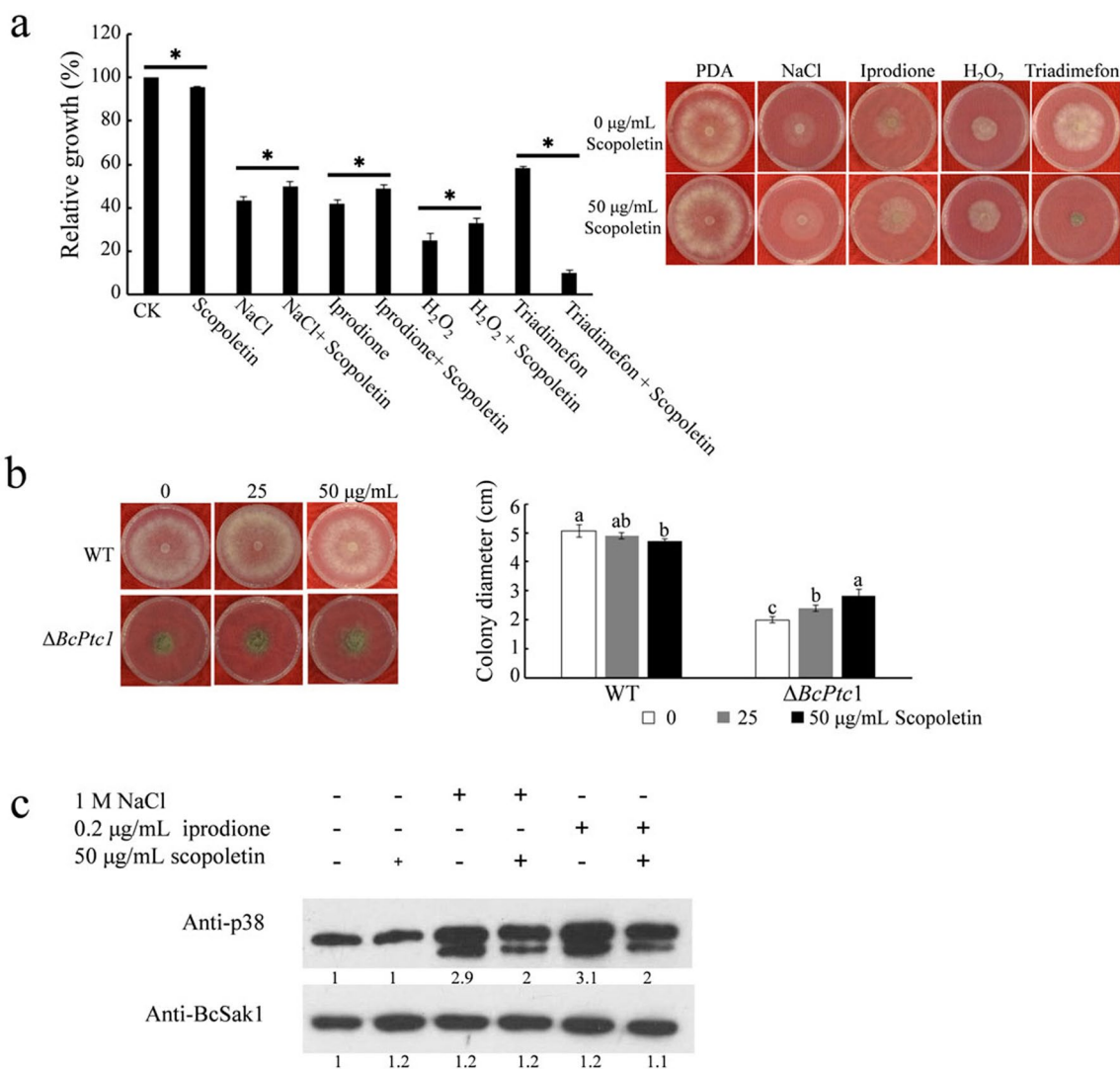
Fig. 5 Scopoletin interferes with the HOG pathway. **a** Sensitivity of B05.10 to 1 M NaCl, 0.2 μg/mL iprodione, 10 mM H_2O_2, and 2 μg/mL triadimefon with/without 50 μg/mL scopoletin. The morphology of the strains was photographed and measured after the plates were incubated at 25℃ for 36 h. *: significant at $P < 0.05$. **b** Morphology of wild-type strain and *BcPtc1* deletion mutant Δ*BcPtc1* with/without 50 μg/mL scopoletin. The morphology of the strains was photographed and measured after the plates were incubated at 25℃ for 36 h. Values on the bars followed by different letters are significantly different at $P = 0.05$. **c** Scopoletin treatment decreases BcSak1 phosphorylation of B05.10 in response to NaCl and iprodione. Fresh mycelia were cultured in PDB broth for 30 h and treated with 1 M NaCl, 0.2 μg/mL iprodione, and 50 μg/mL scopoletin for another 1 h, as indicated in the figure

dehydratase (BcSCD1). Here, four of these genes are downregulated in response to scopoletin, including *BcPKS13* (−1.73), *BcBRN1* (−1.73), *BcBRN2* (−1.53), and *BcSCD1* (−1.68). In addition, no genes involved in melanin biosynthesis are upregulated. Thus, although certain intermediate products of DHN melanin biosynthesis are brown, like scytalone, the dark pigment observed in the study is unlikely to be one of the intermediate products of DHN melanin.

Based on RNA-seq and phosphorylation analysis, scopoletin appears to regulate the HOG pathway in *B. cinerea*. The HOG pathway in fungi can be activated by various stressors, including fungicide treatment, osmotic stress, and exogenous hormone application (Xu 2000; Wang et al 2023). Here, we proved that scopoletin could reduce the phosphorylation level of BcSak1, an ortholog of the yeast HOG1p MAP kinase activated by osmotic stress and dicarboximides.

Table 2 DEGs involved in the virulence of *B. cinerea*

	Gene	Gene_id	Gene description	log$_2$Fold change
1	Bcaba2 (Siewers et al. 2006)	Bcin08g03840	Abscisic acid gene	5.10
2	Bcpme1 (Valette-Collet et al. 2003)	Bcin08g02970	Pectin methylesterase	4.62
3	Bcnep1 (Schouten et al. 2008)	Bcin06g06720	Phytotoxic Nep1-like proteins	4.18
4	Bcrcn1 (Harren et al. 2012)	Bcin09g02820	Regulator calcipressin	3.42
5	BcCHSI (Choquer et al. 2004)	Bcin09g01210	Chitin synthase	3.06
6	BcCrh1 (Bi et al. 2021)	Bcin01g06010	Transglycosylase	2.89
7	*Bcsmr1* (Zhou et al. 2017)	Bcin02g08760	Transcription factor	2.30
8	BcCHSIIIa (Choquer et al. 2004)	Bcin04g03120	Chitin synthase	2.17
9	BcCHSII (Choquer et al. 2004)	Bcin12g01380	Chitin synthase	2.15
10	BcPg2 (Kars et al. 2005)	Bcin14g00610	Endopolygalacturonase	2.05
11	Bccrz1 (Schumacher et al. 2008a)	Bcin01g08230	Calcineurin-responsive zinc finger transcription factor	2.05
12	Bcboa13 (Porquier et al. 2019)	Bcin01g00130	Botcinic acid biosynthesis	1.89
13	Bcpg1 (ten Have et al. 1998)	Bcin14g00850	Endopolygalacturonase	1.89
14	Bcsho1 (Ren et al. 2019)	Bcin08g05150	Membrane spanning proteins	1.65
15	Bcser2 (Liu et al. 2020)	Bcin08g02990	Subtilisin-Like Protease	1.50
16	Bcpdi1 (Marschall and Tudzynski 2017)	Bcin06g05730	Protein Disulfide Isomerase	1.37
17	BcBIR1 (Shlezinger et al. 2011)	Bcin15g04140	Anti-apoptotic	1.37
18	BcactA (Li et al. 2020)	Bcin16g02020	Actin	1.27
19	Bcgar1 (Zhang and van Kan 2013)	Bcin06g04660	D-galacturonic acid catabolism	1.24
20	Bcsod1 (Zhang and van Kan 2013)	Bcin03g03390	Superoxide dismutase	1.20
21	Bmp3 (Rui and Hahn 2007)	Bcin09g02390	MAP kinase	1.17
22	BcCHSVII (Choquer et al. 2004)	Bcin07g01300	Chitin synthase	1.11
23	Bcptc1 (Yang et al. 2013)	Bcin03g01720	Type 2C protein phosphatases	1.10
24	Bcpde1 (Harren et al. 2013)	Bcin10g00450	Phosphodiesterase	−1.01
25	Bcltf1 (Schumacher et al. 2014)	Bcin14g03930	Transcription factor	−1.04
26	Bcap8 (ten Have et al. 2010)	Bcin12g02040	Aspartic proteinase genes	−1.22
27	Bcplc1 (Schumacher et al. 2008b)	Bcin05g02840	Phospholipase C	−1.27
28	Bcreg1 (Michielse et al. 2011)	Bcin07g02530	Transcriptional regulator	−1.27
29	Bcbrn2 (Zhang et al. 2015)	Bcin03g08100	Tetra-hydroxynaphthalene (THN) reductases	−1.53
30	BcatrD (Hayashi et al. 2002)	Bcin13g02720	ABC transporter	−1.55
31	Bcltf3 (Brandhoff et al. 2017)	Bcin11g01720	Light-responsive transcriptional regulator	−1.55
32	Bcscd1 (Zhou et al. 2022)	Bcin03g08110	Melanin biosynthesis gene	−1.68
33	Bcpks13 (Zhang et al. 2015)	Bcin03g08050	Polyketide synthase	−1.73
34	Bcbrn1 (Zhang et al. 2015)	Bcin01g10690	Tetrahydroxynaphthalene (THN) reductases	−1.73
35	Bcnep2 (Schouten et al. 2008)	Bcin02g07770	Phytotoxic Nep1-like proteins	−1.78
36	Bcbck1 (Yin et al. 2018)	Bcin02g06590	MAPK kinase	−1.85
37	Bcfhg1 (Turrion-Gomez et al. 2010)	Bcin04g06230	Flavohemoglobin	−2.13
38	BcAtf1 (Temme et al. 2012)	Bcin09g00920	Transcription factors	−2.22
39	Bcara1 (Nafisi et al. 2014)	Bcin02g07700	Endo-arabinanase	−2.45
40	Bcltf2 (Cohrs et al. 2016)	Bcin16g02090	Transcription factor	−2.52
41	Bcmfs1 (Hayashi et al. 2002)	Bcin01g09910	Major facilitator superfamily transporter	−4.04

Excessive activation of the HOG pathway is the primary antimicrobial mechanism of dicarboximides. Based on our results, scopoletin could interfere with this process, which may reduce the control efficiency of iprodione. The regulation mechanism needs to be further explored in future studies.

Scopoletin was also found to destabilize *B. cinerea* cell walls and cell membranes. Upon treatment with scopoletin, several genes involved in ergosterol biosynthesis were downregulated, including *BcErg1*, *BcErg3*, *BcErg5*, and *BcErg8*. Ergosterol is the major sterol component of fungal membranes and is involved in a variety of cellular

processes, making the ergosterol biosynthesis pathway an attractive antifungal target (Monk et al. 2020). Here, we proved that scopoletin significantly increased the control efficiency of triadimefon. Thus, compared to dicarboximides, DMIs may be a better choice for controlling gray mold on plants that produce scopoletin, like tobacco.

In response to pathogen infection, plants respond with OB and HR, resulting in local cell death blocking pathogen colonization (Mur et al. 2008). To survive, pathogens either need to interfere with host ROS production or enzymatically detoxify ROS. Peroxidases are the enzymes that mediate H_2O_2 detoxification and have evolved to be highly conserved (Yang et al. 2016). In this study, the expression dynamics of 13 peroxidase-related genes (GO:0004601) were significantly altered in response to scopoletin treatment. Furthermore, scopoletin treatment resulted in a significant increase in H_2O_2 accumulation in leaves inoculated with *B. cinerea.* Scopoletin appears to alter ROS homeostasis, leading to an effective gray mold control.

Conclusions

In conclusion, scopoletin is highly effective against *B. cinerea* infection. Specifically, scopoletin can inhibit mycelial growth, conidial germination, and infection structure formation. Scopoletin treatment also had a significant impact on the gene transcription dynamics of *B. cinerea.* This study identified a total of 3495 DEGs, out of which 1285 were upregulated genes and 2210 were downregulated genes. In addition, scopoletin was found to negatively regulate the HOG pathway, destabilize cell walls and cell membranes, and impair ROS homeostasis in *B. cinerea.*

Methods

Fungal and chemical materials

The standard reference strain of *B. cinerea* B05.10 Pers. Fr. [*B. fuckeliana* (de Bary) Whetzel] was used in the study. B05.10 was cultured on PDA (200 g potato infusion, 20 g glucose, 20 g agar, and 1 L water) plates. Scopoletin (Med Chem Express) was dissolved in dimethyl sulfoxide (DMSO).

Fungal growth inhibition assay

The *B. cinerea* B05.10 was cultured on PDA for 3 d, after which fresh mycelial plugs were collected from the edge of the colony and placed on new PDA plates amended with 100, 200, 300, or 500 μg/mL scopoletin. Blank PDA plates were used as a negative control. The cultures were examined after 3 d of incubation at 25℃.

Conidial germination inhibition assay

After 10 d of incubation on PDA plates at 25℃, conidia of *B. cinerea* B05.10 were harvested in 1/2 PDB broth and adjusted to a final concentration of 10^5 conidia/mL. Four different concentrations of scopoletin were applied (50, 100, and 200 μg/mL), and an untreated sample was used as a control. After 7 h of incubation at 25℃ on a hydrophobic glass surface, conidial germination rates were calculated under a microscope. The relative germination inhibition (RGI, %) of conidia was quantified as $[(C-T)/C]\times100$, where T is the conidial germination rate of the treated sample and C is the conidial germination rate of the control sample.

Growth tests

Fresh mycelial plugs taken from the edge of 36 h B05.10 colony were placed on PDA plates amended with or without scopoletin (100, 200, 300, and 500 μg/mL). The cultures were incubated at 25℃ for 3 days before they were examined. The relative inhibition of mycelium growth was quantified as $[(C-T)/C]\times100$, where T is the diameter of the treated strain and C is the diameter of the control strain without scopoletin treatment.

Pathogenicity and infection-related morphogenesis assays

The pathogenicity assay was performed on tomato leaves. Conidia of *B. cinerea* B05.10 were harvested in 1/2 PDB broth and adjusted to a final concentration of 10^5 conidia/mL. Scopoletin was added to the conidia suspension at 50 or 100 μg/mL concentrations. An untreated conidial suspension was used as a negative control. Healthy, unwounded, detached tomato leaves were treated with exactly 15 μL of each conidial suspension. The treated leaves were incubated at 25℃ under 16 h of daylight and 100% humidity for 3 d. All pathogenesis assays were repeated three times.

The infection-related morphogenesis assay was performed on the onion epidermis as previously described (Viaud et al. 2006). For appressorium formation assays, conidia of B05.10 were harvested in 10 mM fructose (with/without scopoletin) to a final concentration of 10^5 conidia/mL. 20 μL conidia mixtures were placed on clean slides and incubated in a moistened chamber at 25℃ for 8 h. For infection cushion formation assays, mycelium plugs were taken from the edge of 48 h old strains, placed on clean slides, and incubated in a moistened chamber at 25℃ for 36 h before being examined under microscope.

Transcriptomic sequencing

From 10-day-old PDA plates, conidia of *B. cinerea* B05.10 were harvested in YEPD medium (0.5% yeast extract, 1% peptone, and 1% glucose) and adjusted to a final

concentration of 10^5 conidia/mL. After 24 h of incubation at 25°C and 180 rpm, samples were amended with 10 μg/mL scopoletin and incubated for 4 h at 25°C prior to harvest. Additional untreated cultures were used as a control, and three independent experiments were performed. Samples were sent to Novogene (Beijing, China) for transcriptomic sequencing (Wu et al. 2015).

Data analysis

The *B. cinerea* B05.10 reference genome was built using Hisat2 v2.0.5, and paired-end reads were aligned to the reference genome. Read assembly, mapping, and FPKM (Fragments Per Kilobase of transcript sequence per Million base pairs sequenced) calculations were carried out as previously described (Xu et al. 2022). The DESeq2 (1.16.1) package was used to analyze differentially expressed genes (DEGs). DEGs with $|\log_2 (\text{fold-change})|>=1$ and padj < 0.05 were considered significant. The clusterProfiler (1.16.1) package was used to perform KEGG and GO enrichment analyses.

Western blotting assay

The cultures were incubated and harvested as described in the section on transcriptomic sequencing. Total protein was extracted as described previously (Yun et al. 2015). Total high osmolarity glycerol 1 (Hog1) (Santa Cruz Biotechnology sc-165978) was used as the reference. The Phospho-p38 MAPK (Thr180/Tyr182) antibody (Cell Signaling Technology) was used to detect the phosphorylation levels of Hog1.

Reverse transcription-quantitative PCR

In order to validate the transcriptomic sequencing results, qRT-PCR was conducted. The $2^{-\Delta\Delta Ct}$ method was used to calculate the gene expression levels (Livak and Schmittgen 2001). The *B. cinerea actin* gene was used as a reference and amplified using the actin-F and actin-R primer pair (Additional file 5: Table S5).

Propidium iodide fluorescence assay

A PI fluorescence assay was conducted to evaluate scopoletin-induced cell membrane damage (Han et al. 2019). Conidia of *B. cinerea* B05.10 were diluted in YEPD medium to a final concentration of 10^5 conidia/mL. After 24 h of incubation at 25°C and 180 rpm, samples were amended with either 50 μg/mL scopoletin or DMSO (control) and incubated for 4 h at 25°C prior to harvest. Cultures were then stained with 2 μM/L PI for 30 min in the dark before being observed and photographed under a fluorescence microscope.

Calcofluor white staining

The samples were collected and treated as described in the PI fluorescence assay, and calcofluor white (CFW) staining was performed as described previously (Rui and Hahn 2007).

Abbreviations

BP	Biological process
CC	Cell components
CFW	Calcofluor white
DEGs	Differentially expressed genes
DHN	Dihydroxynaphthalene
DMIs	Demethylationinhibitors
DMSO	Dimethyl sulfoxide
EC_{50}	Half maximal effective concentration
GO	Gene ontology
HOG	High-osmolarity glycerol
HR	Hypersensitive response
KEGG	Kyoto encyclopedia of genes and genomes
MF	Molecular function
OB	Oxidative burst
PDA	Potato dextrose agar
PKS	Polyketide synthases
PI	Propidium iodide
RNA-seq	RNA sequencing
ROS	Reactive oxygen species
RT-qPCR	Reverse transcription quantitative PCR

Supplementary Information

The online version contains supplementary material available at https://doi.org/10.1186/s42483-023-00219-4.

Additional file 1: Table S1. Summary of reads from scopoletin-treated (BSco) and untreated (BCK) *B. cinerea*.

Additional file 2: Table S2. 3495 differentially expressed genes (DEGs) of *B. cinerea* in response to 10 μg/mL scopoletin.

Additional file 3: Table S3. Gene Ontology (GO) enrichment analysis of 3495 DEGs.

Additional file 4: Table S4. Kyoto Encyclopedia of Genes and Genomes (KEGG) pathway enrichment analysis of 3495 DEGs.

Additional file 5: Table S5. Gene description and their primers used in the study.

Yuan *et al. Phytopathology Research*   (2024) 6:1

Page 13 of 14

Availability of data and materials

The datasets generated in the current study are available in NCBI repository: https://www.ncbi.nlm.nih.gov/bioproject/PRJNA877049.

Declarations

Ethics approval and consent to participate

Not applicable.

Consent for publication

Not applicable.

Competing interests

The authors declare that they have no competing interests.

References

Adnan M, Hamada MS, Hahn M, Li GQ, Luo CX. Fungicide resistance of *Botrytis cinerea* from strawberry to procymidone and zoxamide in Hubei. China Phytopathol Res. 2019;1:17. https://doi.org/10.1186/s42483-019-0024-8.

Antika LD, Tasfiyati AN, Hikmat H, Septama AW. Scopoletin: a review of its source, biosynthesis, methods of extraction, and pharmacological activities. Z Naturforsch C J Biosci. 2022;77:303–16. https://doi.org/10.1515/znc-2021-0193.

Beyer SF, Beesley A, Rohmann PFW, Schultheiss H, Conrath U, Langenbach CJG. The Arabidopsis non-host defence-associated coumarin scopoletin protects soybean from Asian soybean rust. Plant J. 2019;99:397–413. https://doi.org/10.1111/tpj.14426.

Bi K, Scalschi L, Jaiswal N, Mengiste T, Fried R, Sanz AB, et al. The *Botrytis cinerea* Crh1 transglycosylase is a cytoplasmic effector triggering plant cell death and defense response. Nat Commun. 2021;12:2166. https://doi.org/10.1038/s41467-021-22436-1.

Brandhoff B, Simon A, Dornieden A, Schumacher J. Regulation of conidiation in *Botrytis cinerea* involves the light-responsive transcriptional regulators BcLTF3 and BcREG1. Curr Genet. 2017;63:931–49. https://doi.org/10.1007/s00294-017-0692-9.

Carpinella MC, Ferrayoli CG, Palacios SM. Antifungal synergistic effect of scopoletin, a hydroxycoumarin isolated from *Melia azedarach* L. fruits. J Agric Food Chem. 2005;53:2922–7. https://doi.org/10.1021/jf0482461.

Choquer M, Boccara M, Gonçalves IR, Soulié MC, Vidal-Cros A. Survey of the *Botrytis cinerea* chitin synthase multigenic family through the analysis of six euascomycetes genomes. Eur J Biochem. 2004;271:2153–64. https://doi.org/10.1111/j.1432-1033.2004.04135.x.

Cohrs KC, Simon A, Viaud M, Schumacher J. Light governs asexual differentiation in the grey mould fungus *Botrytis cinerea* via the putative transcription factor BcLTF2. Environ Microbiol. 2016;18:4068–86. https://doi.org/10.1111/1462-2920.13431.

Costet L, Fritig B. Kauffmann S (2002) Scopoletin expression in elicitor-treated and tobacco mosaic virus-infected tobacco plants. Physiol Plant. 2002;115:228–35. https://doi.org/10.1034/j.1399-3054.2002.1150208.x.

El Oirdi M, Trapani A, Bouarab K. The nature of tobacco resistance against *Botrytis cinerea* depends on the infection structures of the pathogen. Environ Microbiol. 2010;12:239–53. https://doi.org/10.1034/j.1399-3054.2002.1150208.x.

Federica Zaninotto SLC, Annalisa P, Delledonne M. Cross talk between reactive nitrogen and oxygen species during the hypersensitive disease resistance response. Plant Physiol. 2006;141:379–83. https://doi.org/10.1104/pp.106.078857.

Fillinger S, Elad Y. *Botrytis*—the Fungus, the pathogen and its management in agricultural systems. Berlin: Springer; 2016. p. 413–86.

Han XB, Zhao J, Cao JM, Zhang CS. Essential oil of *Chrysanthemum indicum* L.: potential biocontrol agent against plant pathogen P*hytophthora nicotianae*. Environ Sci Pollut Res Int. 2019;26:7013–23. https://doi.org/10.1007/s11356-019-04152-y.

Harren K, Brandhoff B, Knödler M, Tudzynski B. The high-affinity phosphodiesterase BcPde2 has impact on growth, differentiation and virulence of the phytopathogenic ascomycete *Botrytis cinerea*. PLoS ONE. 2013;8: e78525. https://doi.org/10.1371/journal.pone.0078525.

Harren K, Schumacher J, Tudzynski B. The Ca^{2+}/calcineurin-dependent signaling pathway in the gray mold *Botrytis cinerea*: the role of calcipressin in modulating calcineurin activity. PLoS ONE. 2012;7: e41761. https://doi.org/10.1371/journal.pone.0041761.

Hayashi K, Schoonbeek HJ, De Waard MA. Bcmfs1, a novel major facilitator superfamily transporter from *Botrytis cinerea*, provides tolerance towards the natural toxic compounds camptothecin and cercosporin and towards fungicides. Appl Environ Microbiol. 2002;68:4996–5004. https://doi.org/10.1128/AEM.68.10.4996-5004.2002.

Kars I, Krooshof GH, Wagemakers L, Joosten R, Benen JA, van Kan JA. Necrotizing activity of five *Botrytis cinerea* endopolygalacturonases produced in *Pichia pastoris*. Plant J. 2005;43:213–25. https://doi.org/10.1111/j.1365-313X.2005.02436.x.

Lemos ASO, Florêncio JR, Pinto NCC, Campos LM, Silva TP, Grazul RM, et al. Antifungal activity of the natural coumarin scopoletin against planktonic cells and biofilms from a multidrug-resistant *Candida tropicalis* strain. Front Microbiol. 2020;11:1525. https://doi.org/10.3389/fmicb.2020.01525.

Li H, Zhang Z, Qin G, He C, Li B, Tian S. Actin is required for cellular development and virulence of *Botrytis cinerea* via the mediation of secretory proteins. eSystems. 2020;5:e00732-19-e819. https://doi.org/10.1128/mSystems.00732-19.

Liu W, Leroux P, Fillinger S. The HOG1-like MAP kinase Sak1 of *Botrytis cinerea* is negatively regulated by the upstream histidine kinase Bos1 and is not involved in dicarboximide- and phenylpyrrole-resistance. Fungal Genet Biol. 2008;45:1062–74. https://doi.org/10.1016/j.fgb.2008.04.003.

Liu X, Xie J, Fu Y, Jiang D, Chen T, Cheng J. The Subtilisin-like protease Bcser2 affects the sclerotial formation, conidiation and virulence of *Botrytis cinerea*. Int J Mol Sci. 2020;21:603. https://doi.org/10.1128/mSystems.00732-19.

Livak KJ, Schmittgen TD. Analysis of relative gene expression data using real-time quantitative PCR and the $2^{-\Delta\Delta CT}$ method. Methods. 2001;25:402–8. https://doi.org/10.1006/meth.2001.1262.

Mur LAJ, Kenton P, Lloyd AJ, Ougham H, Prats E. The hypersensitive response; the centenary is upon us but how much do we know? J Exp Bot. 2008;59:501–20. https://doi.org/10.1093/jxb/erm239.

Marschall R, Tudzynski P. The protein disulfide isomerase of *Botrytis cinerea*: an ER protein involved in protein folding and redox homeostasis influences NADPH oxidase signaling processes. Front Microbiol. 2017;8:960. https://doi.org/10.3389/fmicb.2017.00960.

Michielse CB, Becker M, Heller J, Moraga J, Collado IG, Tudzynski P. The *Botrytis cinerea* Reg1 protein, a putative transcriptional regulator, is required for pathogenicity, conidiogenesis, and the production of secondary metabolites. Mol Plant Microbe Interact. 2011;24:1074–85. https://doi.org/10.1094/MPMI-01-11-0007.

Monk BC, Sagatova AA, Hosseini P, Ruma YN, Wilson RK, Keniya MV. Fungal lanosterol 14α-demethylase: a target for next-generation antifungal design. Biochim Biophys Acta Proteins Proteom. 2020;1868: 140206. https://doi.org/10.1016/j.bbapap.2019.02.008.

Nafisi M, Stranne M, Zhang L, van Kan JA, Sakuragi Y. The endo-arabinanase BcAra1 is a novel host-specific virulence factor of the necrotic fungal phytopathogen *Botrytis cinerea*. Mol Plant Microbe Interact. 2014;27:781–92. https://doi.org/10.1094/MPMI-02-14-0036-R.

Parra C, Soto E, León G, Salas CO, Heinrich M, Echiburú-Chau C. Nutritional composition, antioxidant activity and isolation of scopoletin from *Senecio nutans*: support of ancestral and new uses. Nat Prod Res. 2018;32:719–22. https://doi.org/10.1080/14786419.2017.1335726.

Porquier A, Moraga J, Morgant G, Dalmais B, Simon A, Sghyer H, et al. Botcinic acid biosynthesis in *Botrytis cinerea* relies on a subtelomeric gene cluster surrounded by relics of transposons and is regulated by the Zn_2Cys_6 transcription factor BcBoa13. Curr Genet. 2019;65:965–80. https://doi.org/10.1007/s00294-019-00952-4.

Ren W, Liu N, Yang Y, Yang Q, Chen C, Gao Q. The sensor proteins BcSho1 and BcSln1 are involved in, though not essential to, vegetative differentiation, pathogenicity and osmotic stress tolerance in *Botrytis cinerea*. Front Microbiol. 2019;10:328. https://doi.org/10.3389/fmicb.2019.00328.

Rui H. The Slt2-type MAP kinase Bmp3 of *Botrytis cinerea* is required for normal saprotrophic growth, conidiation, plant surface sensing and host tissue

colonization. Mol Plant Pathol. 2007;8(2):173–84. https://doi.org/10.1111/j.1364-3703.2007.00383.x.

Schouten A, Van Baarlen P, Van Kan JAL. Phytotoxic Nep1-like proteins from the necrotrophic fungus *Botrytis cinerea* associate with membranes and the nucleus of plant cells. New Phytol. 2008;177:493–505. https://doi.org/10.1111/j.1469-8137.2007.02274.x.

Schumacher J, de Larrinoa IF, Tudzynski B. Calcineurin-responsive zinc finger transcription factor CRZ1 of *Botrytis cinerea* is required for growth, development, and full virulence on bean plants. Eukaryot Cell. 2008a;7:584–601. https://doi.org/10.1128/EC.00426-07.

Schumacher J, Simon A, Cohrs KC, Viaud M, Tudzynski P. The transcription factor BcLTF1 regulates virulence and light responses in the necrotrophic plant pathogen *Botrytis cinerea*. PLoS Genet. 2014;10: e1004040. https://doi.org/10.1371/journal.pgen.1004040.

Schumacher J, Viaud M, Simon A, Tudzynski B. The Galpha subunit BCG1, the phospholipase C (BcPLC1) and the calcineurin phosphatase co-ordinately regulate gene expression in the grey mould fungus *Botrytis cinerea*. Mol Microbiol. 2008b;67:1027–50. https://doi.org/10.1111/j.1365-2958.2008.06105.x.

Shaw CY, Chen CH, Hsu CC, Chen CC, Tsai YC. Antioxidant properties of scopoletin isolated from *Sinomium acutum*. Phytother Res. 2003;17:823–5. https://doi.org/10.1002/ptr.1170.

Shlezinger N, Minz A, Gur Y, Hatam I, Dagdas YF, Talbot NJ, et al. Anti-apoptotic machinery protects the necrotrophic fungus *Botrytis cinerea* from host-induced apoptotic-like cell death during plant infection. PLoS Pathog. 2011;7: e1002185. https://doi.org/10.1371/journal.ppat.1002185.

Siewers V, Kokkelink L, Smedsgaard J, Tudzynski P. Identification of an abscisic acid gene cluster in the grey mold *Botrytis cinerea*. Appl Environ Microbiol. 2006;72:4619–26. https://doi.org/10.1128/AEM.02919-05.

Sun H, Wang L, Zhang B, Ma J, Hettenhausen C, Cao G, et al. Scopoletin is a phytoalexin against *Alternaria alternata* in wild tobacco dependent on jasmonate signalling. J Exp Bot. 2014;65:4305–15. https://doi.org/10.1093/jxb/eru203.

Temme N, Oeser B, Massaroli M, Heller J, Simon A, Collado IG, et al. BcAtf1, a global regulator, controls various differentiation processes and phytotoxin production in *Botrytis cinerea*. Mol Plant Pathol. 2012;13:704–18. https://doi.org/10.1111/j.1364-3703.2011.00778.x.

ten Have A, Espino JJ, Dekkers E, Van Sluyter SC, Brito N, Kay J, et al. The *Botrytis cinerea* aspartic proteinase family. Fungal Genet Biol. 2010;47:53–65. https://doi.org/10.1016/j.fgb.2009.10.008.

ten Have A, Mulder W, Visser J, van Kan JA. The endopolygalacturonase gene Bcpg1 is required for full virulence of *Botrytis cinerea*. Mol Plant Microbe Interact. 1998;11:1009–16. https://doi.org/10.1094/MPMI.1998.11.10.1009.

Thompson JE, Fahnestock S, Farrall L, Liao DI, Valent B, Jordan DB. The second naphthol reductase of fungal melanin biosynthesis in *Magnaporthe grisea*: tetrahydroxynaphthalene reductase. J Biol Chem. 2000;275:34867–72. https://doi.org/10.1074/jbc.M006659200.

Turrion-Gomez JL, Eslava AP, Benito EP. The flavohemoglobin BCFHG1 is the main NO detoxification system and confers protection against nitrosative conditions but is not a virulence factor in the fungal necrotroph *Botrytis cinerea*. Fungal Genet Biol. 2010;47:484–96. https://doi.org/10.1016/j.fgb.2010.03.001.

Valette-Collet O, Cimerman A, Reignault P, Levis C, Boccara M. Disruption of *Botrytis cinerea* pectin methylesterase gene Bcpme1 reduces virulence on several host plants. Mol Plant Microbe Interact. 2003;16:360–7. https://doi.org/10.1094/MPMI.2003.16.4.360.

Viaud M, Fillinger S, Liu W, Polepalli JS, Le PP, Kunduru AR, et al. A class III histidine kinase acts as a novel virulence factor in *Botrytis cinerea*. Mol Plant Microbe Interact. 2006;19:1042–50. https://doi.org/10.1094/MPMI-19-1042.

Wang J, Wen Z, Chen Y, Ma ZH. The sucrose non-fermenting-1 kinase Snf1 is involved in fludioxonil resistance via interacting with the high osmolarity glycerol MAPK kinase Hog1 in *Fusarium*. Phytopathol Res. 2023;5:52. https://doi.org/10.1186/s42483-023-00208-7.

Williamson B, Tudzynski B, Tudzynski P, van Kan JA. *Botrytis cinerea*: the cause of grey mould disease. Mol Plant Pathol. 2007;8:561–80. https://doi.org/10.1111/j.1364-3703.2007.00417.x.

Wu H, Wei L, Fan F, Ji S, Zhang S, Geng J, et al. Integration of Hippo signalling and the unfolded protein response to restrain liver overgrowth and tumorigenesis. Nature Commun. 2015;6:6239. https://doi.org/10.1038/ncomms7239.

Xu JR. Map kinases in fungal pathogens. Fungal Genet Biol. 2000;31:137–52. https://doi.org/10.1006/fgbi.2000.1237.

Xu Y, Wang Y, Wang L, Liang W, Yang Q. Sodium valproate is effective against *Botrytis cinerea* infection of tomato by enhancing histone H3 acetylation-directed gene transcription and triggering tomato fruit immune response. Phytopathology. 2022;112:1264–72. https://doi.org/10.1094/PHYTO-11-21-0483-R.

Yang Q, Jiang J, Mayr C, Hahn M, Ma Z. Involvement of two type 2C protein phosphatases BcPtc1 and BcPtc3 in the regulation of multiple stress tolerance and virulence of *Botrytis cinerea*. Environ Microbiol. 2013;15:2696–711. https://doi.org/10.1111/1462-2920.12126.

Yang SL, Yu PL, Chung KR. The glutathione peroxidase-mediated reactive oxygen species resistance, fungicide sensitivity and cell wall construction in the citrus fungal pathogen *Alternaria alternata*. Environ Microbiol. 2016;18:923–35. https://doi.org/10.1111/1462-2920.13125.

Yin D, Wu S, Liu N, Yin Y, Ma Z. The natural fenhexamid-resistant grey mould populations from strawberry in Zhejiang Province are dominated by *Botrytis cinerea* group S. Pest Manag Sci. 2016;72:1540–8. https://doi.org/10.1002/ps.4183.

Yin Y, Wu S, Chui C, Ma T, Jiang H, Hahn M, et al. The MAPK kinase BcMkk1 suppresses oxalic acid biosynthesis via impeding phosphorylation of BcRim15 by BcSch9 in *Botrytis cinerea*. PLoS Pathog. 2018;14: e1007285. https://doi.org/10.1371/journal.ppat.1007285.

Yun Y, Liu Z, Yin Y, Jiang J, Chen Y, Xu JR, et al. Functional analysis of the *Fusarium graminearum* phosphatome. New Phytol. 2015;207:119–34. https://doi.org/10.1111/nph.13374.

Zhang C, He Y, Zhu P, Chen L, Wang Y, Ni B, et al. Loss of bcbrn1 and bcpks13 in *Botrytis cinerea* not only blocks melanization but also increases vegetative growth and virulence. Mol Plant Microbe Interact. 2015;28:1091–101. https://doi.org/10.1094/MPMI-04-15-0085-R.

Zhang L, van Kan JA. *Botrytis cinerea* mutants deficient in D-galacturonic acid catabolism have a perturbed virulence on *Nicotiana benthamiana* and Arabidopsis, but not on tomato. Mol Plant Pathol. 2013;14:19–29. https://doi.org/10.1111/j.1364-3703.2012.00825.x.

Zhao W, Li C, Liang J, Sun S. The *Aspergillus fumigatus* β-1,3-glucanosyltransferase Gel7 plays a compensatory role in maintaining cell wall integrity under stress conditions. Glycobiology. 2014;24:418–27. https://doi.org/10.1093/glycob/cwu003.

Zhou Y, Song J, Wang Y, Yang L, Wu M, Li G, et al. Biological characterization of the melanin biosynthesis gene Bcscd1 in the plant pathogenic fungus *Botrytis cinerea*. Fungal Genet Biol. 2022;160: 103693. https://doi.org/10.1016/j.fgb.2022.103693.

Zhou Y, Yang L, Wu M, Chen W, Li G, Zhang J. A single-nucleotide deletion in the transcription factor gene bcsmr1 causes sclerotial-melanogenesis deficiency in *Botrytis cinerea*. Front Microbiol. 2017;8:2492. https://doi.org/10.3389/fmicb.2017.02492.